

# Rapid Disappearance of Penumbra-Like Features Near a Flaring Polarity Inversion Line: The Hinode Observations

B. Ravindra<sup>1</sup> and Sanjay Gosain<sup>2,3</sup>

<sup>1</sup>Indian Institute of Astrophysics, Koramangala, Bangalore - 560034, India

<sup>2</sup>Udaipur Solar Observatory, Dewali, Badi Road, Udaipur - 313001, India

<sup>3</sup>National Solar Observatory, 950 N Cherry Avenue, Tucson 85719 AZ, USA

**Abstract:** We present the observations of penumbra like features (PLFs) near a polarity inversion line (PIL) of flaring region. The PIL is located at the moat boundary of active region (NOAA 10960). The PLFs appear similar to sunspot penumbrae in morphology but occupy small area, about  $6 \times 10^7 \text{ km}^2$ , and are not associated with sunspot or pore. We observed a rapid disappearance of the PLFs after a C1.7 class flare, which occurred close to the PIL. The local correlation tracking (LCT) of these features shows presence of horizontal flows directed away from the end-points of the PLFs, similar to the radial outward flow found around regular sunspots, which is also known as the moat flow. Hard X-ray emission, coincident with the location of the PLFs, is found in RHESSI observations, suggesting a spatial correlation between the occurrence of the flare and decay of the PLFs. Vector magnetic field derived from the observations obtained by Hinode spectro-polarimeter SOT/SP instrument, before and after the flare, shows a significant change in the horizontal as well as the vertical component of the field, after the flare. The weakening of both the components of the magnetic field in the flare interval suggests that rapid cancellation and/or submergence of the magnetic field in PLFs occurred during the flare interval.

## 1 Introduction

Well developed sunspots have umbra surrounded by elongated filamentary type of structures called penumbral filaments. The magnetic field in the umbra is mostly vertical to the solar surface while in the penumbra it is horizontally inclined. Further, the inclination of the penumbral magnetic field shows an azimuthal variation, with channels of more horizontal field lying in between the channels of more vertical fields. This alternating inclination of penumbral field is also called as “uncombed penumbra” and is well established from the past observations (Solanki and Montavan, 1993). The more horizontal component of the uncombed field is observed to harbor most of the Evershed flow. Penumbrae form around pores abruptly with an increase in the magnetic field inclination at the boundary (Tildesley and Weiss, 2004). Penumbral filament formation and Evershed flow occurs nearly simultaneously in pores (Leka and Skumanich, 1998), i.e., as soon as the penumbrae form the Evershed flow can be observed. It is found that a magnetic flux threshold above which penumbra forms is about  $1\text{-}1.5 \times 10^{20} \text{ Mx}$  (Leka and Skumanich, 1998).

Once the penumbra is formed it survives from hours to days exhibiting a variety of small

scale structures like dark cores inside penumbral filaments, apparently propagating twisting structures, moving magnetic features to name a few. Evershed flow (Evershed, 1909), a mass flow directed radially outwards from the sunspot along the penumbra is observed in the photosphere, while inverse Evershed flow, directed towards sunspot is observed in the chromosphere. The actual lifetime of the penumbra depends upon the life of the sunspot, when the spot decays it gradually loses its penumbra, becomes a “naked” sunspot and finally fragments into pores. Moving Magnetic Features (MMFs: Harvey and Harvey, 1973) are proposed as one of the candidates for the decay of sunspots. Once the sunspot decays, naturally the penumbra disappears. Decay of sunspots is studied in detail by Martinez Pillet (2002) and found that not all MMFs are related to the decay of sunspots. Bellot Rubio et al. (2008) have found that the absence of Evershed flow in penumbral field lines can raise the penumbral filaments to the chromosphere that can cause the disappearance of the penumbra at the photospheric level. Large flares can also cause the disappearance of the penumbra at the outer boundary of the sunspots (Wang et al. 2004; Sudol and Harvey 2005). It is believed that the field becomes more vertical at the outer edge of sunspot as the overall active region field collapses towards the flaring PIL (Gosain 2012), which causes disappearance of penumbrae.

In this paper, we report on new type of penumbra like features (PLFs) that are not associated with sunspot. Further, we use LCT method to study the horizontal flow patterns around these structures. We then study the evolution of PLFs in the photosphere, chromosphere and in vector magnetograms using the space based data obtained from Hinode/SOT and find that the structure rapidly disappears during flare. In the forthcoming sections, we present details of the G-band, Ca II H, spectro-polarimetric data and its analysis. This is followed by the observational results on the disappearance of PLFs. Possible explanation for the flare related disappearance of PLFs is discussed in the last section.

## 2 Data and Analysis

The space based telescope, Solar Optical Telescope (SOT: Tsuneta et al., 2008) onboard Hinode, obtains images of the Sun at an unprecedented resolution of about  $0.2''$  of the photosphere and chromosphere. The broadband filter imager (BFI) instrument on the SOT produces images in several wavelengths with the 3-8 Å bandwidth filters. In this study, we have used filtergrams observed at 4305 Å (G-band) and 3968.5 Å (Ca II H). We have used the filtergrams observed in these wavelengths from June 06, 2007 at 15:00 UT to June 07, 2007 05:00 UT. The data are corrected for dark current, pixel-to-pixel gain variations, hot and dead pixels. The Ca II H data are corrected for the wavelength dependent pixel size with the G-band as a reference. These calibrated data sets are rigidly aligned with the first image in the time series using a 2-dimensional cross-correlation algorithm. The alignment of the images is good to a sub-pixel accuracy. The aligned data sets are passed through a subsonic filter with a cutoff value of  $4 \text{ km s}^{-1}$  to remove the effect of acoustic oscillations (Title, et al. 1989).

The spectro-polarimeter (SOT/SP: Ichimoto, et al. 2008) instrument is one of the back-end instruments of SOT onboard Hinode satellite, makes maps of the active region by spatial scanning and obtains Stokes I, Q, U and V spectra in Fe I 6301.5 and 6302.5 Å lines. A fast-mode raster scan with 980 steps at a step size of 0.295'' along the scanning direction and 0.317''/pixel resolution along the slit direction made a raster image with a field-of-view of about 290''×162''. The Stokes signals are calibrated using standard SolarSoft pipeline for SP. The magnetic fields are obtained by using an inversion scheme based on the Milne-Eddington algorithm (Skumanich and Lites 1987; Lites and Skumanich 1990). The ambiguity in the azimuth is resolved based on the minimum energy algorithm (Metcalf, 1994; Leka et al. 2009). Later, the magnetic field vector has been transformed to the disk center (Venkatakrishnan et al., 1989). The resulting vertical ( $B_z$ ) and transverse ( $B_t$ ) magnetic fields have measurement errors of 8 G and 30 G, respectively. These magnetograms are used to study the magnetic field parameters of the PLFs.

### 3 Results

We focus our study on the small scale penumbra like feature located at the moat boundary of the active region NOAA 10960 observed from 6-7th June, 2007. The AR NOAA 10960 consists of two large sunspots of negative polarity, a plage region of positive polarity, and several pores of either polarity (<http://www.solarmonitor.org>). Two sunspots were aligned along the East-West direction at a latitude of 6° in the southern hemisphere. During our observations of event, the active region was close to the disk center (S06E05). Active Region NOAA 10960 produced several B and C class flares with a very few M class flares and the largest one was observed on June 04, 2007 which was of M8.9 class. A few of these events were studied in detail by Srivastava et al. (2010) and Kumar et al. (2010), where they have observed the sunspot rotation and kink instability that lead to the initiation of the flare. During Hinode observations, there was one C1.7 class flare on June 06, 2007 at 23:31 UT and it occurred close to the polarity inversion line (PIL marked in Figure 2). On June 07, 2007 between 00:00 to 05:00 UT there were two B-class flares and their magnitude was B7.6 and B6.6 peaking at 00:45 and 01:40 UT respectively. This event was well observed by the Hinode/SOT at high cadence (21 sec.) in Ca II H band with some small data gaps in-between. It was also observed in G-band at a slower cadence of about 100 sec.

Figure 1 (top) and (bottom) shows the sunspot in the active region at the photospheric and chromospheric level. Penumbra like features (PLFs) are observed close to the sunspot and it is marked with a box. An enlarged portion of boxed region is shown next to it. Close to the PLFs region, three pores are visible which are quite separated from the PLFs and are not like the pores which form rudimentary penumbra. The same structure is also visible in the chromospheric image taken in Ca II H wavelength. The region of interest is shown in box is magnified and displayed along side. Clearly, in the magnified image one can see detailed view of the PLFs. They exhibit about 10'' linear size and appear very much like the sunspot penumbra. The AR 10960 was a fast evolving region and started to disrupt from June 04, 2007 (see: [http://solar-b.nao.ac.jp/QLmovies/movie\\_sirius/2007/06/04/hsc\\_ql20070604\\_e.shtml](http://solar-b.nao.ac.jp/QLmovies/movie_sirius/2007/06/04/hsc_ql20070604_e.shtml)).

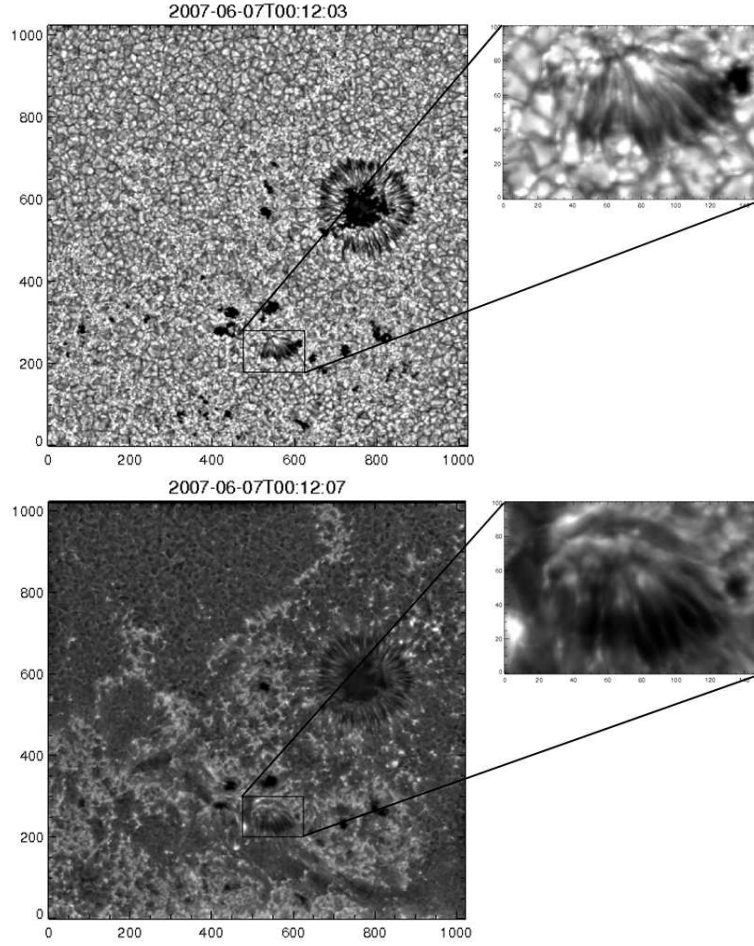


Figure 1: Top: A sample image is obtained from Hinode/SOT using G-band filter. The boxed region shows the region of interest. A magnified view of the region of interest is shown on the right side of it. Bottom: Same as top side image but obtained in the wavelength of  $3968 \text{ \AA}$  of Ca II H. The scales are in unit of pixel.

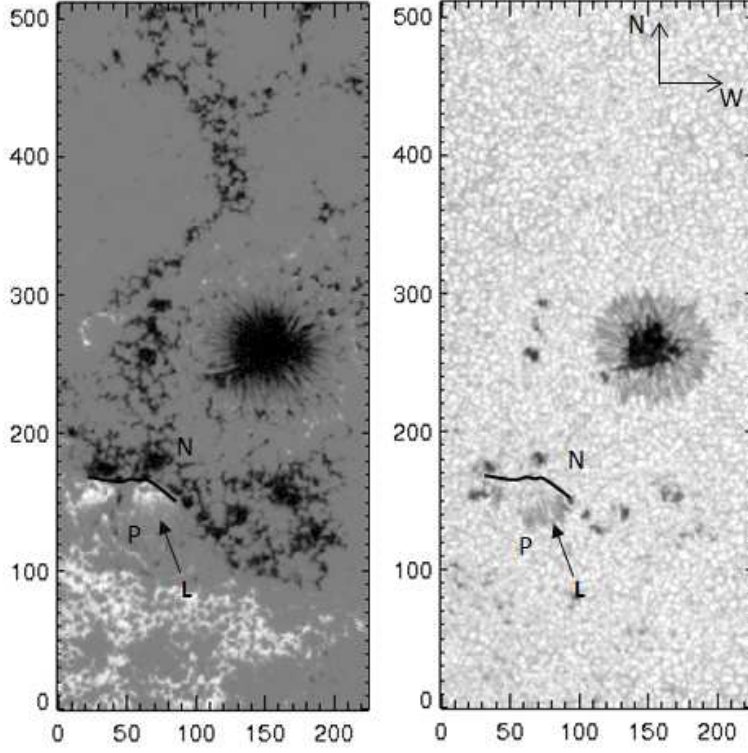


Figure 2: A map of line-of-sight component of the magnetic field (left) and the corresponding continuum image (right) obtained from spectro-polarimeter onboard Hinode on June 06, 2007 at 22:57 UT. The arrow indicates the position of PLFs. P and N represents the positive and negative polarity regions. A dark line between negative and positive polarity represents the position of the polarity inversion line. The scales are in unit of pixel.

The formation process of the PLFs could not be clearly identified as the cadence of the observations is intermittent and the field-of-view of Hinode SOT is also limited. However, here we concentrate more on two aspects (i) brief investigation of the properties of the new PLFs identified in Hinode G-band observations, and (ii) their evolution in relation to recurrent flares. The search for the origin or formation of PLFs would require a fully dedicated high resolution observational campaign, which we plan to do in near future either with Hinode SOT or ground based high resolution telescopes equipped with adaptive-optics.

Interestingly, the PLFs are located next to the polarity inversion line (PIL) with PLFs filaments aligned nearly parallel to the PIL (Figure 2). In Figure 2 the left side image is the line-of-sight magnetogram and the right side image is the continuum image. Both the images are obtained from SOT/SP. A thin dark line in-between the positive and negative polarity is shown to represent the position of the PIL. Close to this PIL numerous B and C-class flares were observed over a couple of days. The PLFs (location ‘L’, shown by an



arrow in Figure 2) has positive polarity and is located close to the PIL. Here, the magnetic field in the lower part of PLFs (close to the arrow-head) is more inclined leading to smaller signal in line-of-sight component of the magnetic fields. In the magnetogram, it is very clear that the region PLFs is located in the moat boundary of the negative polarity sunspot.

### 3.1 Evolution of the PLFs

The evolution of the PLFs at the photospheric and chromospheric level is depicted in Figure 3. The PLFs in G-band and Ca II H images are shown alternatively for near simultaneous time intervals. On June 06, at 16:00 UT the PLFs is clearly visible in the photospheric as well as in the chromospheric images. The PLFs appears to have very small pore at one end and, however, compared to the size of PLFs it is very tiny, so the origin of PLFs cannot be this tiny pore. Later, at 00:30 UT on June 07, 2007 it reduced its size drastically and at 01:30 UT a small remnant of it is visible in the photospheric images. A similar type of evolution is observed in the chromospheric images, except that some brightening can also be seen close to the PIL on June 7, 2007.

### 3.2 Temporal correlation

We then measured the area of the PLFs quantitatively starting from 15:00 UT of June 06, 2007. The area of the PLFs is measured from the G-band images. We adopted the following methodology to measure the area of the PLFs. We first smooth the image by  $0.9'' \times 0.9''$  pixel box to remove any small scale intensity variations in the time sequence of images. This small scale variations in the intensity of images could occur due to residual oscillations after filtering and residual flat-fielding errors. We then pick the pixels whose values smaller than 0.6 times the value of the quiet sun intensity in the photosphere. This criteria is same for all the images. This method clearly picks the dark regions that contain not only the PLFs but also the pore regions. To select only the PLFs region we then labeled the regions which assigns a unique number to the individual detected sub-regions. We use ‘label\_region.pro’ function of IDL data analysis platform to do the labeling. Using this technique we isolated the PLFs from rest of the region. Once the PLFs region has been isolated, by counting the number of pixels we estimated the area of the PLFs. The variation of PLF’s area as a function of time is shown in Figure 4. We have also plotted the GOES X-ray flux below the areal plot for easy comparison. In the plot, we have drawn the vertical lines to show the peak time of the three flares which are observed close to the PIL. We notice the following features in the evolutionary trend: (i) The PLFs area is almost constant, about  $6 \times 10^7 \text{ km}^2$  before the C1.7-class flare (first flare), that is, between 22:13 to 23:31 UT on June 06, 2007. (ii) The PLFs area started to decrease during the C1.7-class flare and it reduced to almost 3/4th of its original size during the B7.6 class flare (second flare). (iii) After the B6.6-class flare (third flare) the size of the PLFs reduced drastically and eventually the entire PLFs disappeared. Thus, from these observations it is clear that the decrease of PLFs area is co-temporal with the duration of three recurrent flares which are closely spaced in time and

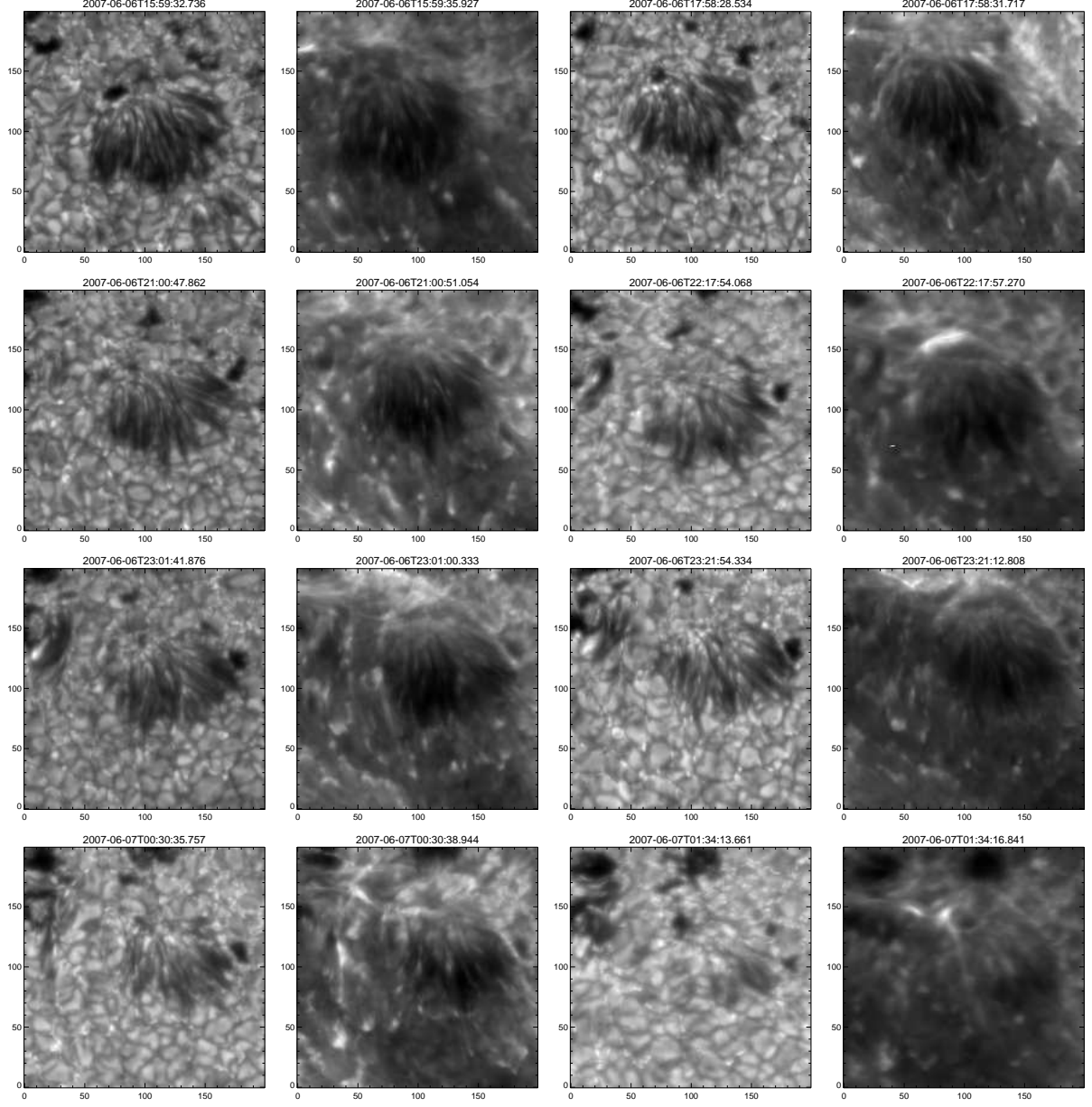


Figure 3: The temporal evolution of the PLFs is shown in sequence of G-band and Ca II H images alternatively. The date and time of the image acquisition is shown on the top of each image. The numbers on the axes represent the pixel.

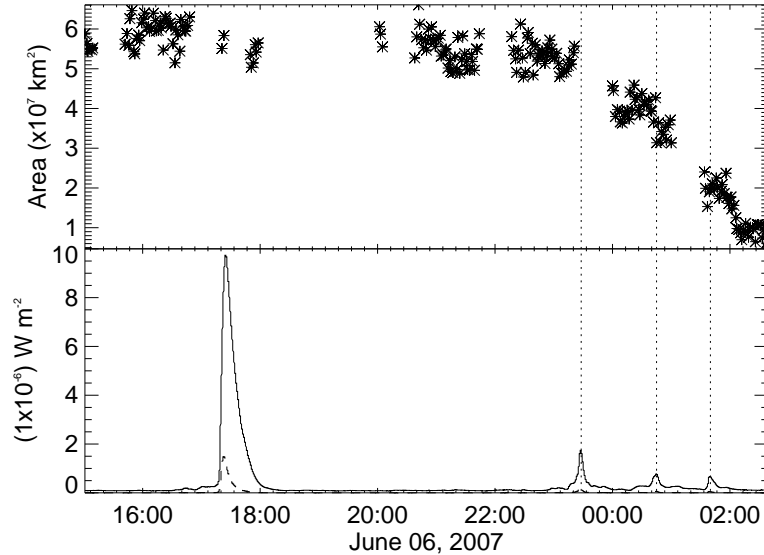


Figure 4: Top: The area of the PLFs is plotted as a function of time. Bottom: The GOES X-ray flus is plotted as a function of time. The dotted vertical lines from left to right side represent the peak time of C1.7, B7.6 and B6.6 class flares respectively.

located along the same PIL. The PLFs disappeared in about 2 hours after it starts to decay. There are data gaps in between the observations, however a decreasing trend in PLFs area can be easily recognized. In section 3.4 we also study the spatial correlation between the flare brightening and the location of PLFs using co-aligned RHESSI X-ray images. These observations suggest co-spatiality between these PLFs and the flare emission in X-ray. We discuss the possible relation in section 4.

### 3.3 Flow fields in the PLFs

The penumbrae associated with the sunspots exhibit an outflow and inflow that appear to be originate from the mid portion of the penumbra (Ravindra, 2006). In general there is a radial outflow pattern around sunspots which is also known as the moat flow. From high resolution observations it was found that these radial outflows in the moat region appear only when penumbrae are present and are not seen in those parts of irregular sunspots where penumbrae are missing (Vargas Domnguez et al. 2007). In order to examine the flows in and around the PLFs we computed the horizontal flow fields using the local correlation tracking (LCT: November and Simon, 1988) technique. Figure 5 shows the flow fields in the PLFs region. The left side image shows the flow field on June 06, before the C1.7 class flare (first flare) and the right side image is obtained after the B6.6 class flare (third flare). In the left side image, the PLFs exhibits an outward flow which appears to be originating in the mid portion of the PLFs. The flow is in general, directed away from the PLFs, a little similar to



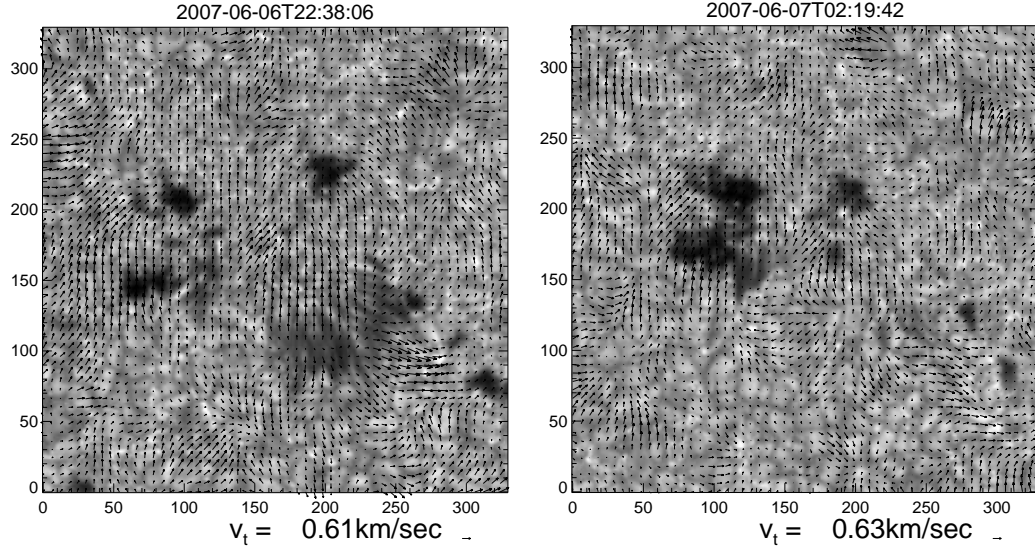


Figure 5: The horizontal velocity vectors overlaid upon G-band image showing the PLFs. Left: Image acquired before the C1.7 class flare. Right: Image acquired after the PLFs decay.

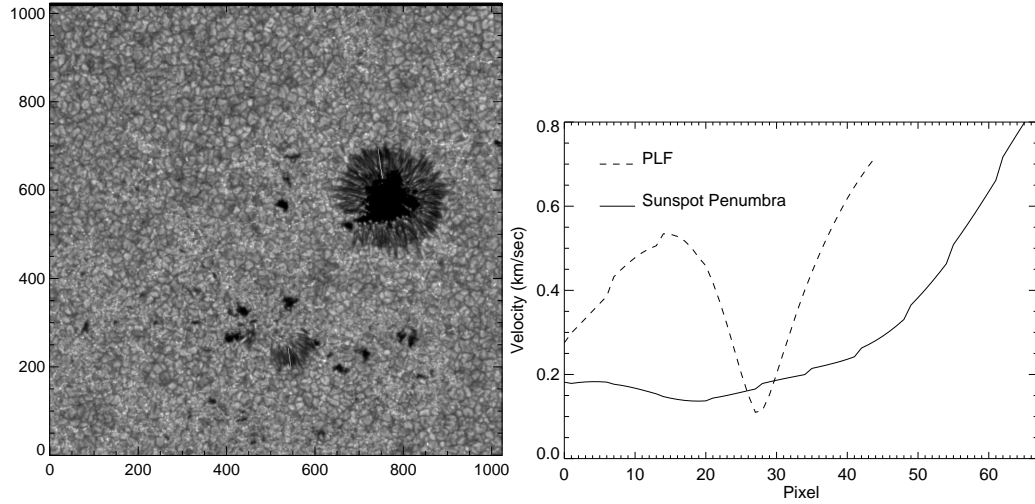


Figure 6: Left: The location of the velocities extracted for the penumbra associated with the sunspot and the PLF is shown with white line. Right: The velocity for penumbral region and PLF region is plotted.

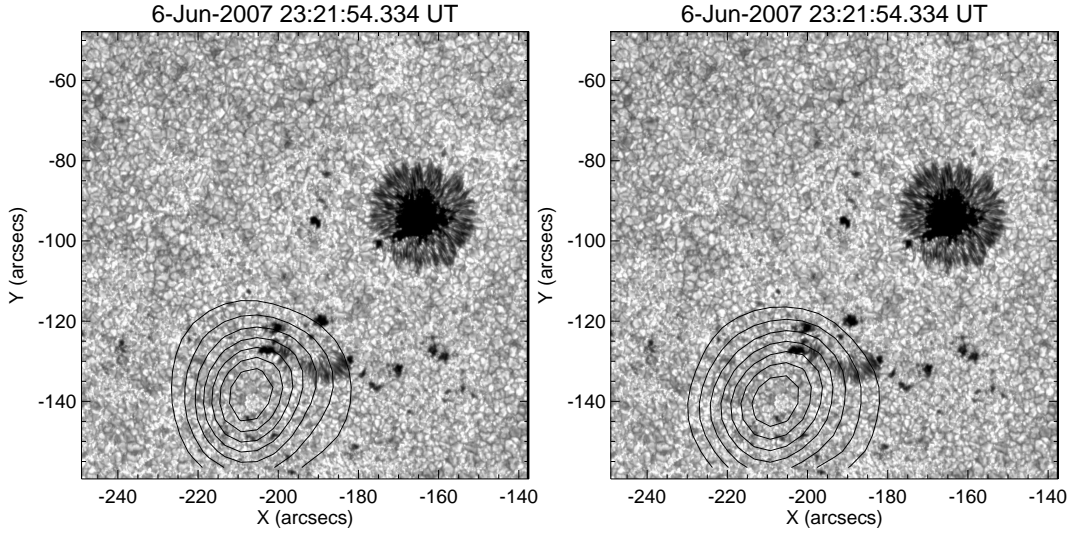


Figure 7: The contours of the RHESSI hard X-ray images overlaid upon the G-band images. Left: The contours of 6 to 12 keV and Right: 12 to 25 keV.

what one finds around sunspots. However, here the PLFs is not in a radial symmetry like sunspots and hence the associated flows are also non-symmetric. On the right side image, we notice that at the location where the PLFs disappeared, we can observe a supergranular like outward flow pattern which is roughly of the same size as that of the PLFs.

In order to compare the flow fields in the PLFs with the penumbral filaments we selected one region on the PLF and another on the sunspot penumbra, as shown in Figure 6(left) with a white line. The LCT velocities are compared for both the regions and is shown in Figure 6(right). The velocity in the penumbra which is directed towards the umbra is small, about  $0.2 \text{ km s}^{-1}$  and after the mid penumbra towards the outer penumbra the velocity increases. This result is similar to the observations of Sobotka, Brandt and Simon (1999). The velocity is large near the outer penumbra, about  $0.8 \text{ km s}^{-1}$ . On the other hand the velocity in PLFs increases on either side of mid portion of the PLF and it is minimum of about  $0.2 \text{ km s}^{-1}$  in the mid portion of the PLF. This suggests that there are diverging flows from the middle portion of PLFs. Clearly then there is a difference in the transverse field flow patterns in the PLF with respect to penumbra associated with sunspot.

### 3.4 Spatial correlation

Hard X-ray flux is the indicator of the footpoint of the source of flare ribbons in the chromosphere (Masuda, Kosugi, and Hudson, 2001). It also represents the thermal and non-thermal footpoints of the loops during micro-flares (Hannah, Krucker, Hudson, Christe, and Lin, 2008). We overlaid the contours of hard X-ray fluxes in the energy range from 6-12 and 12-25 keV from RHESSI on to the G-band images. As the pointing is known to be good for

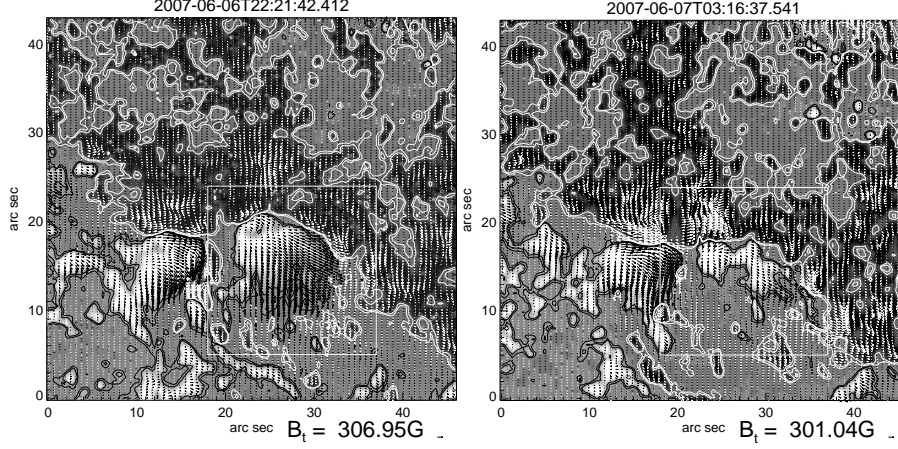


Figure 8: Transverse field vectors overlaid upon the vertical component of the magnetic field. Left side images are obtained before the C1.7 class flare and the right side images are obtained after the PLFs decay.

the MDI, the G-band images were co-aligned with the MDI intensity images by overlying the contours of MDI intensity image on the G-band image. The contours of hard X-ray from RHESSI is overlaid on the co-aligned HINODE G-band images (Figure 7). This kind of low resolution RHESSI contours overlaid upon the hi-resolution G-band and SOT/NFI images has been successfully used to locate the footpoints of the reconnecting loops in the corona (e. g. Matthews, Zharkov, and Zharkova, 2011; Watanabe et al. 2010). The left side image shows the contour maps for the 6-12 keV energy range and the right side is for 12-25 keV range. These contours were plotted for the 40, 50, 60, 70, 80 and 90% of the maximum counts in the corresponding hard X-ray images. An observation of these contour maps show that the contours are mainly concentrated near the region of PLFs suggesting the spatial correlation between the flare location and the PLFs.

### 3.5 Vector Field Maps

Figure 8 (left) and (right) shows the vector magnetic fields before and after the flares, respectively. The vector maps show an overlay of the horizontal component of the magnetic field (represented by arrows, where the length of the arrow is proportional to the magnitude of the horizontal field and the direction tells the direction of the horizontal field) upon the vertical magnetic fields (represented as gray scale image with overlaid contours). In the map, the boxed region shows the PLFs location and the contours are drawn at  $\pm 50$  and  $100$  G levels of the  $B_z$  component of the magnetic fields. Comparison shows that the  $B_z$  and  $B_t$  component of the magnetic field in the PLFs location decreased substantially after the flare.

Figure 9 shows the histogram representing the distribution of  $B_z$  and  $B_t$  components of the magnetic fields in the region of PLFs. The left and right side plots show the distributions

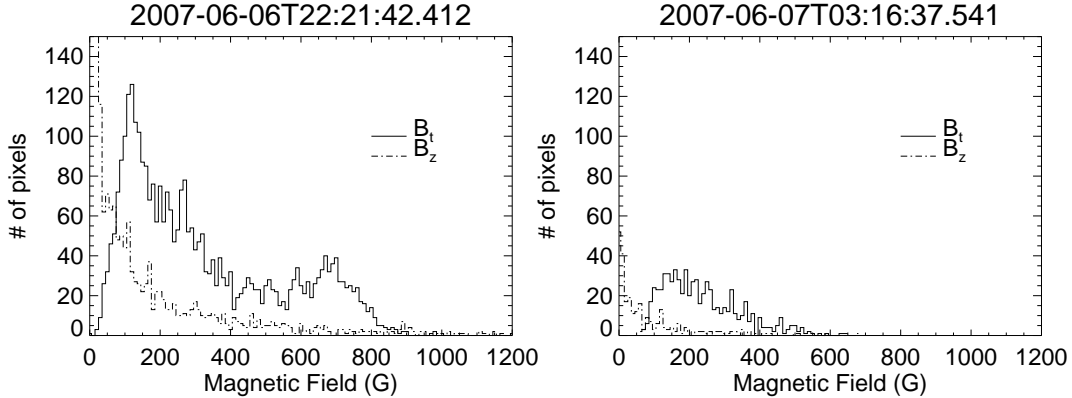


Figure 9: Left: Histogram of the vertical component ( $B_z$ ) and transverse component of the magnetic fields ( $B_t$ ) are plotted for the PLFs obtained an hour before the flare. Right: Same as the left side plot, but for the data obtained about two hours after the flare. The thick line corresponds to the histogram of transverse field strength and the dash dotted line corresponds to the histogram of vertical magnetic field strength.

before and after the flare. The plot shows that a large amount of  $B_t$  component is present in PLFs before the flare and it decreased substantially after the flare. A similar result is found for the  $B_z$  component of the magnetic fields. Before the flare the  $B_z$  and  $B_t$  components of the field in PLFs extended its tail up to 1200 G. After the flare its strength has been reduced to less than half of its value. This suggests that the magnetic field itself has decreased in this region.

## 4 Discussion

We have focused on a new type of magnetic features in the photosphere near the PIL of a flaring active region, which we call as penumbra-like features (PLFs). These PLFs could be observed due to high spatial resolution of Hinode SOT. These features are interesting in the sense that they are not associated with a pore or sunspot. It is generally seen that as pores grow larger they develop penumbrae abruptly, sometimes called rudimentary penumbrae which eventually develop as full sunspot penumbrae if the magnetic flux in the pore continues to grow. More detailed study of these features utilizing high-resolution imaging as well as spectro-polarimetry would shed more light on the formation and evolution of these features along with the magnetic and thermodynamic properties of these features. Also, it is important to know what is the vertical structure of these features, are these shallow or deep rooted, do they harbor similar Evershed flows and show similar uncombed magnetic structure as in sunspot penumbrae? Such a study is currently underway using Hinode SOT/SP and FG instruments and we plan to present the detailed observational characteristics of these



features in a separate paper.

Here we focused on the disappearance of the PLFs in association with the occurrence of three recurrent flares near the PIL where PLFs were located. The PLFs area was about  $6 \times 10^7$  km<sup>2</sup> initially and reduced rapidly during the interval of three flares suggesting a correlation between the occurrence of the flare and the decay of the closely located PLFs. The location of the hard X-ray flux obtained from the RHESSI coincides with the location of the PLFs suggesting that the footpoints of the reconnecting loops in the corona are rooted in or close to the PLFs. The vector magnetic field associated with PLFs shows that these are largely transverse magnetic fields. A comparison of vector magnetic field retrieved by the Stokes inversion of SP data before and after the flares shows that there is a substantial decrease in the transverse as well as vertical field component at the location of the PLFs.

Due to the lack of long time sequence of observations it is difficult to tell exactly how the PLFs were formed. We can think of two possibilities: (i) Since PLFs are found in the location of decaying sunspot it could be the remnant of the sunspot wherein the sunspot got disrupted and a cluster of penumbra got separated from the decaying sunspot. However, this picture does not conform to the typical observations of sunspot decay, where the sunspot loses its penumbral area gradually becoming so-called naked sunspot and resembling a pore, while the penumbrae are lost completely i.e., they do not form PLFs in general, (ii) It could also happen that these are formed independently due to clustering of highly inclined fields near the PIL. Generally the PILs are observed to have strong horizontal fields and often harbor twisted fields (as evidenced in twisted filament structures lying along PIL. The twisted morphology becomes obvious when they erupt as helical structures). At present we can not confirm or rule out either of these possibilities, however, we hope future high resolution observations would help us to gain more knowledge about the formation of the PLFs.

The decay of PLF after the flare could be due to two main reasons, (i) change in field inclination from horizontal to vertical, and (ii) flux cancellation and/or submergence. In the former case we expect the vertical magnetic flux to increase after the flare, which is not observed in the vector magnetograms. Also, if PLFs field becomes vertical then we should see appearance of pores at the location of PLFs, which is not seen in the images. Thus, we can rule out this possibility. The vector magnetic field observations by Hinode SOT/SP however, show a substantial decrease in the magnetic field in the PLFs area, which suggests that the decay of PLFs could be due to the flux cancellation and/or submergence. Since, we do not have a continuous vector magnetic field measurement it is very difficult to conclude firmly upon this. A future continuous high resolution data is therefore required.

In the past the disappearance of penumbra have been observed in large X and M-class flares. The high-resolution Hinode images gave us opportunity of observing the changes in the photosphere even for the small flares with small penumbra like regions (PLFs). We could detect the changes in the area of the decaying PLFs during flare interval, but there is still a lack of vector magnetic field data at high temporal cadence to make more detailed study of the evolution of magnetic field in PLFs. Vector magnetograms from recently launched Solar Dynamic Observatory hold promise to the studies of vector magnetic field evolution of such



small features.

## 5 Acknowledgments

We thank the anonymous referee for constructive suggestions and comments on the paper. Hinode is a Japanese mission developed and launched by ISAS/JAXA, collaborating with NAOJ as a domestic partner, NASA and STFC (UK) as international partners. Scientific operation of the Hinode mission is conducted by the Hinode science team organized at ISAS/JAXA. This team mainly consists of scientists from institutes in the partner countries. Support for the post-launch operation is provided by JAXA and NAOJ (Japan), STFC (U.K.), NASA, ESA, and NSC (Norway).

## References

- [1] Bellot Rubio, L. R., Tritschler, A., and Martinez Pillet, V. 2008 *ApJ*, **676**, 703.
- [2] Evershed, J. 1909, *MNRAS*, **69**, 454.
- [3] Gosain, S., 2012, *ApJ*, In. Press, <http://arxiv.org/abs/1202.1784v1>
- [4] Hannah, I. G., Krucker, S., Hudson, H. S., Christe, S., and Lin, R. P., 2008, *Astron. Astrophys.*, **481**, 45.
- [5] Harvey, K. and Harvey, J., 1973, *Sol. Phys.*, **28**, 61.
- [6] Ichimoto, K. Lites, B., Elmore, D., Suematsu, Y. et al. 2008, *Sol. Phys.*, **249**, 233.
- [7] Kumar, Pankaj, Srivastava, A. K., Filippov, B., Uddin, Wahab, 2010, *Sol. Phys.*, **266**, 39.
- [8] Leka, K. D. and Skumanich, A. 1998, *ApJ*, **507**, 454.
- [9] Leka, K.D., Barnes, G., and Crouch, A. 2009, in *ASP Conf. Ser. 415, The Second Hinode Science Meeting: Beyond Discovery Toward Understanding*, ed. B. Lites, M. Cheung, T. Magara, J. Mariska, and K. Reeves (San Francisco, CA: ASP), 365
- [10] Lites, B. W. and Skumanich, A., 1990, *ApJ*, **348**, 747.
- [11] Martinez Pillet, V. 2002, *Astron. Nachr.*, **323**, 342.
- [12] Masuda, S., Kosugi, T. and Hudson, H. S., 2001, *Sol. Phys.*, **204**, 55.

- [13] Matthews, S. A., Zharkov, S., Zharkova, V. V., 2011, *ApJ*, **739**, 71.
- [14] Metcalf, T. R., 1994, *Sol. Phys.*, **155**, 235
- [15] November, L. J. and Simon, G. W. 1988, *ApJ*, **333**, 427.
- [16] Ravindra, B. 2006, *Sol. Phys.*, **237**, 297.
- [17] Skumanich, A. and Lites, B. W. 1987, *ApJ*, **322**, 473.
- [18] Sobotka, M., Brandt, P. N., Simon, G. W., 1999, *A&A*, **348**, 621.
- [19] Solanki, S. K. and Montavon, C. A. P., 1993, *A&A*, **275**, 283.
- [20] Srivastava, A. K., Zaqarashvili, T. V., Kumar, Pankaj, Khodachenko, M. L., 2010, *ApJ*, **715**, 292.
- [21] Sudol, J. J. and Harvey, J. W. 2005, *ApJ*, **635**, 647.
- [22] Tildesley, M. J. and Weiss, N. O. 2004, *MNRAS*, **350**, 657.
- [23] Title, A. M., Tarbell, T. D., Topka K. P., Ferguson, S. H., Shine, R. A., SOUP Team., 1989, *ApJ*, **336**, 475.
- [24] Tsuneta, S. et al. 2008, *Sol. Phys.*, **58**, 149.
- [25] Vargas Domínguez, S., Bonet, J. A., Martínez Pillet, V., Katsukawa, Y., Kitakoshi, Y. and Rouppe van der Voort, L., 2007, *ApJ*, **660**, 165.
- [26] Venkatakrishnan, P., Hagyard, M. J., and Hathaway, D. H. 1989, *Sol. Phys.*, **122**, 215.
- [27] Wang, H., Liu, C., Qiu, J., Deng., N., Goode, P. R. and Denker, C. 2004, *ApJ*, **601**, 195.
- [28] Watanabe, K., Krucker, S., Hudson, H., Shimizu, T., Masuda, S., and Ichimoto, K., 2010, *ApJ*, **715**, 651.